Magnetic Resonance Imaging

(June 11, 1996)

Instructor: Tai-huang Huang
Institute of Biomedical Sciences
Academia Sinica
Tel. (02) 2652-3036; Fax. (02) 2788-7641
E. mail: bmthh@ibms.sinica.edu.tw

Reference:

1. Stark, D.D. and Bradley, W.G. eds. (1996)
   "Magnetic Resonance Imaging" 2nd ed. Mosby Year Book.
2. Edelman, R.R. and Hesselink, J.R. eds. (1990)
   "Clinical Magnetic Resonance Imaging" Saunders Co.
3. Ernst, E.R., Bodenhausen, G. and Wokaun, A. (1987) Clarendon Press, Oxford.
   "Principles of Nuclear Magnetic Resonance in One and Two Dimensions"

Outlines:

I. Principles on Nuclear Magnetic Resonance Imaging (MRI):

a. Basic NMR Theory: Larmor Equation, Chemical shift, Relaxation phenomenon.

b. Basic Theory of Magnetic Resonance Imaging: Effect of magnetic gradient field, Slice selection, 2D Spin-warp imaging method, phase encoding, frequency encoding, Nyquist theorem, sensitivity, artifacts, fast imaging, angiography, chemical shift imaging.

II. MRI Instrumentation

Magnet, Gradient system, RF system, RF coil and Computer system.

III. Applications

Brain, Head, Neck, Spine, Body, Musculoskeletal system etc.

1. 2. Imaging Methods:

a. Spatial Localization of the MR Signal

In a homogeneous field, the spatial information is lost unless one can collimate the RF-Field as one can with light, but this is not possible.

{ Image: Detection of magnetization (proton, water) as a function of x,y and z. M(x.y.z)

b. Effect of magnetic field gradient:

$B(x) = B_0 + \vec{G}(x, y, z)\Delta\vec{R}(x, y, z)$

$\Rightarrow f(x,y,z) = rB_0 + r(\vec{G} \bullet \vec{R})$ (still a Larmor equation)

$\Rightarrow$ The spatial information is stored in the frequency

$\Rightarrow$ Intensity at certain frequency is correlated to the proton density at a particular spatial location

$\Rightarrow$ Multidimensional NMR spectrum differs from real proton image only by a constant scalar fator

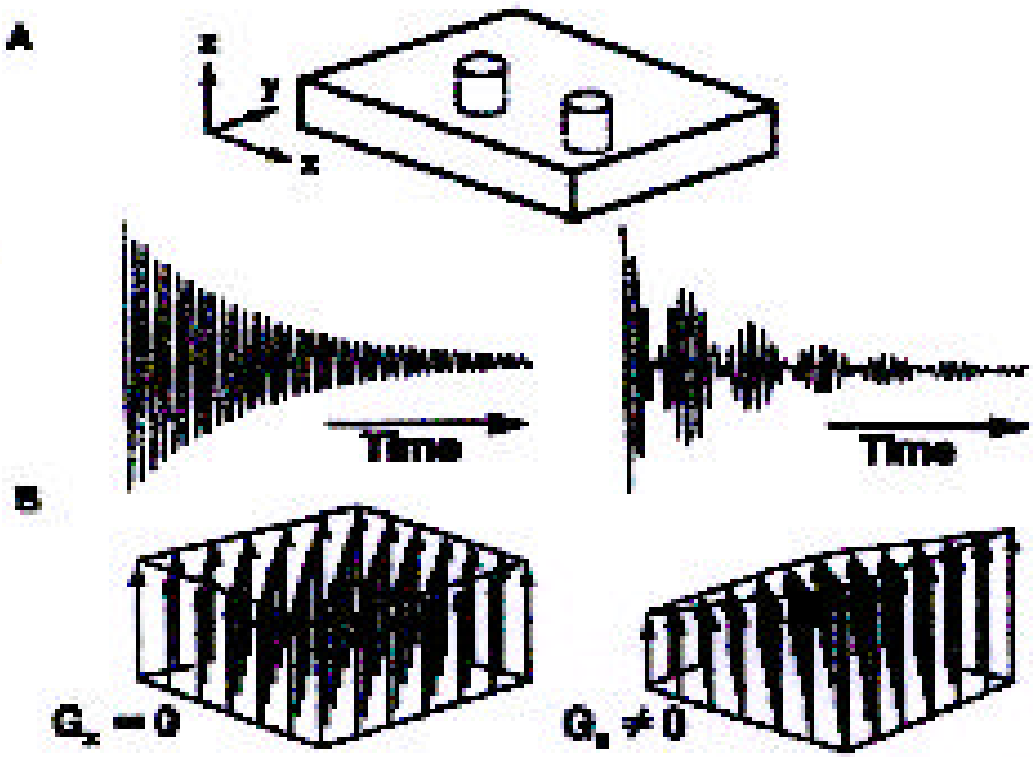


Figure 17. A, In the absence of the field gradient ($G_x = G_y = G_z = 0$) both samples sense the same field; the free induction decay therefore consists of a single frequency. B, In the presence of

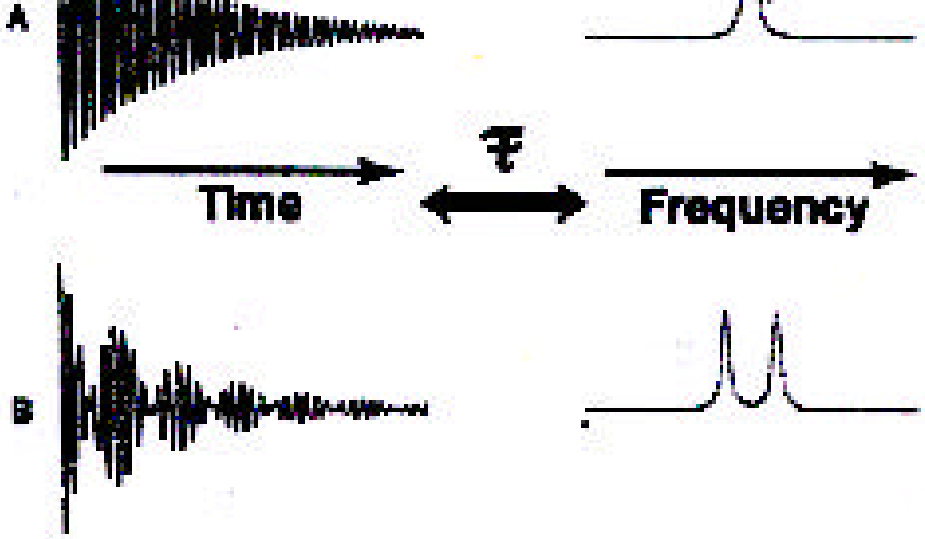


Figure 7-5. Free induction decay and its frequency domain analog for A, a single frequency and B, two different frequencies. The symbol *F* implies that the two domains are related by a Fourier transformation.

Proton Density: The number of MR visible protons in a unit volume of tissue (ρ). ρ is expressed as a percentage of the proton density of water. Vary very little among various tissues.

TABLE 2. PROTON DENSITY, T_1, AND T_2 AS A FUNCTION OF MAGNETIC FIELD STRENGTH

Tissue	T_1 0.2 T*	T_1 0.3 T†	T_1 1.4 T‡	T_1 2.4 T§	T_2	Proton Density (%)
Fat	240	—	—	279	60	9.6
Gray matter	—	—	764	—	88	10.6
White matter	—	380	560	—	72	10.6
Cerebrospinal fluid (CSF)	—	1155	1527	—	140	10.8
Liver	380	—	—	570	40	9.7
Muscle	400	—	—	1023	50	9.3
Spleen	420	—	—	701	20	9.8
Pancreas	290	—	—	605	60	9.8
Bone marrow	—	320	—	554	—	—

*From Rupp, Reiser, Stetter: Eur J Radiol 3:68–76, 1983.
†From Wehrli FW, MacFall JR, Newton TH: Parameters determining the appearance of NMR images. *In* Newton TH, Potts DG (eds): Advanced Imagi
echniques. Vol II. San Anselmo, CA, Clavadel Press, 1983.
‡From Wehrli et al: *In* Peterson SB, et al (eds): An Introduction of Biomedical NMR. New York, Thieme, 1985.
§From Damadian R, Zaner K, Hor D, Di Maio T: Human tumors detected by NMR. Proc Natl Acad Sci USA 71:1471, 1974.

MRI is a versatile, multi-parameter technique.

➔ Different nuclei (Primarily proton, in fact water).

➔ Different chemical shift (Chemical shift imaging).

➔ Relaxation time, T1 and T2

T_1: Decay alone Z-axis.
The time it takes to relax back to Z-axis after perturbation.

T_2: The time it takes to lose phase coherence on X-Y plane.
The time it takes to lose signal on detection.

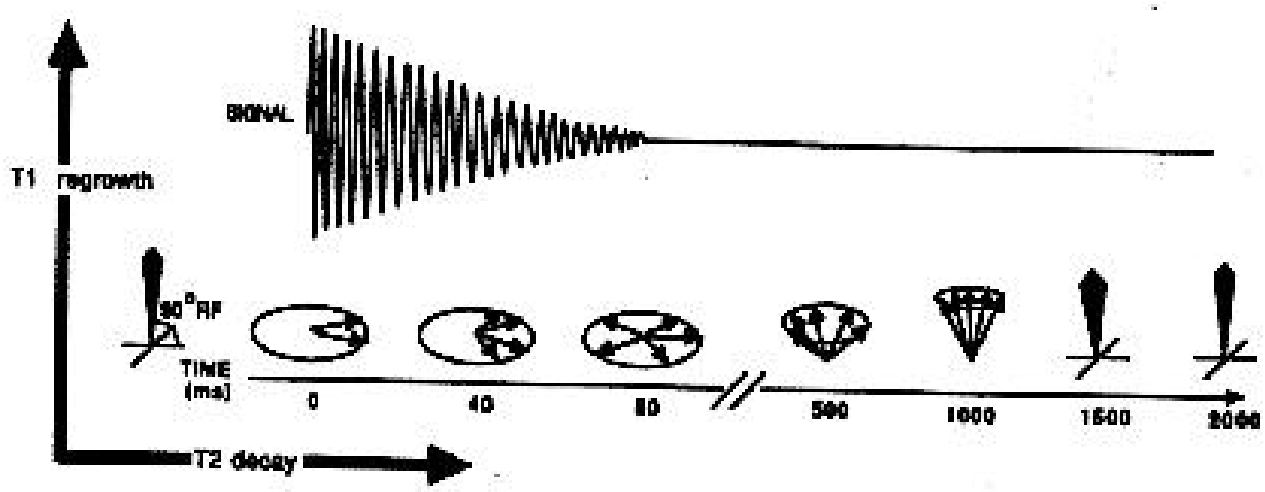


FIGURE . T_1 relaxation and T_2 relaxation are simultaneous processes. Note that T_2 relaxation is completed much more rapidly than T_1 relaxation.

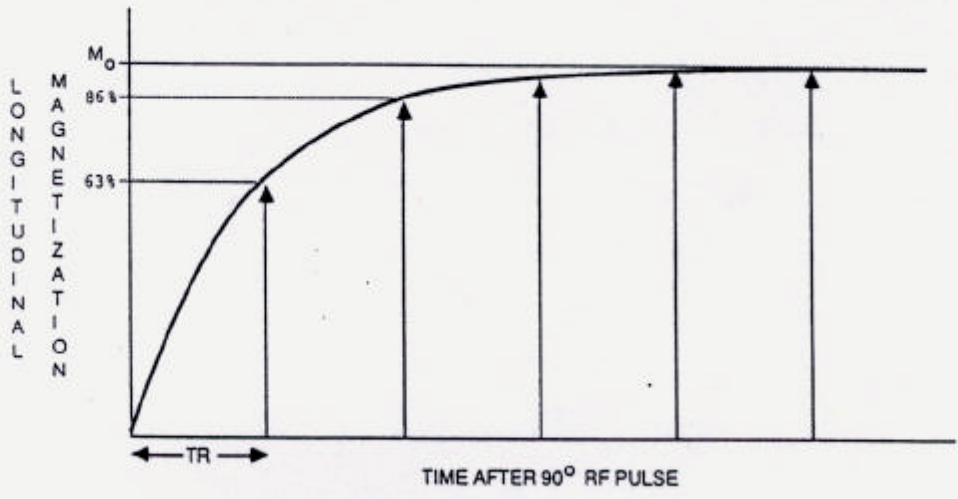


FIGURE 9. . Longitudinal magnetization versus time after a 90-degree RF pulse. The longitudinal magnetization regrows toward the maximal value (M_0) at a rate determined by the T_1 relaxation time.

(Magnetization recovers faster for shorted T_1 sample)

(Magnetization Losses faster for shorter T_2 sample)

❋T_1 and T_2 depends on: (1) Molecular motion (correlation time 2)
(2) Magnetic field strength
(3) Type of nucleus

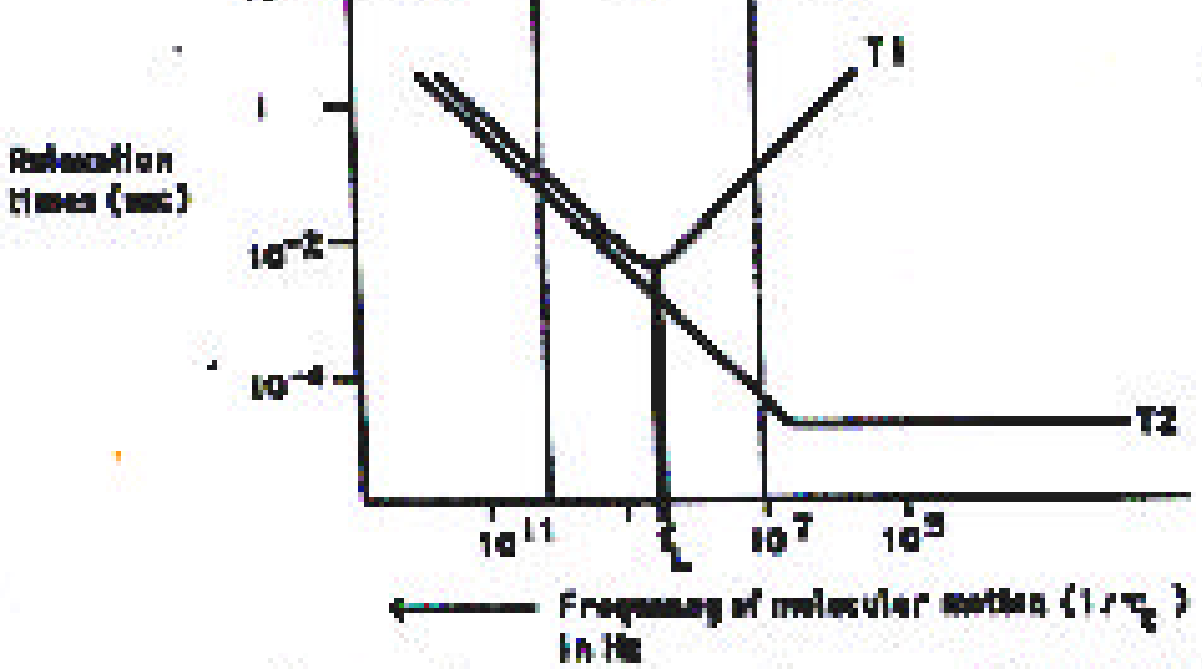


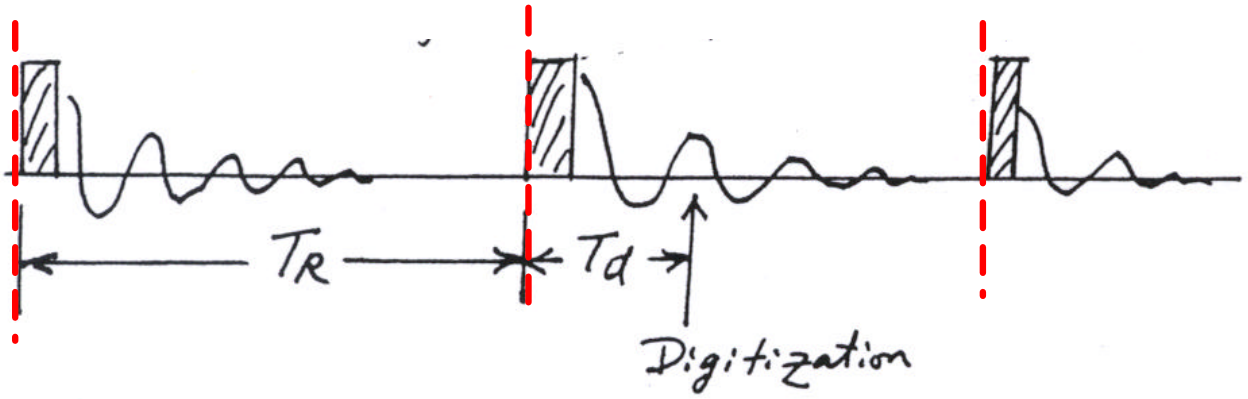
FIGURE 14f. Relaxation time versus frequency of molecular motion ($1/\nu_c$). Free water has rapid diffusion and long T_1 and T_2 times (region A). Bound water associated with restricted motion has shorter T_1 and T_2 times (region B). Very restricted motion results in very-short T_2 times (region C). f_L = Larmor frequency.

Table 1 .. Relaxation times for different brain tissues*

Organ	T1 (ms)	T2 (ms)
Putamen	747 ± 33	71 ± 4
Caudate nucleus	822 ± 16	76 ± 4
Thalamus	703 ± 34	75 ± 4
Cortical gray matter	871 ± 73	87 ± 2
Corpus callosum	509 ± 39	69 ± 6
Superficial white matter	515 ± 27	74 ± 5
Internal capsule	559 ± 18	67 ± 7
Cerebrospinal fluid (lateral ventricle)	1900 ± 353	250 ± 3

*Determined at 1.4 T field strength from a 5 mm slice at the level of the lateral ventricles

What will happen if we vary T_r or T_D ?



T_R: Pulse repetition time.
T_d: Time between end of the pulse and the start of detection.

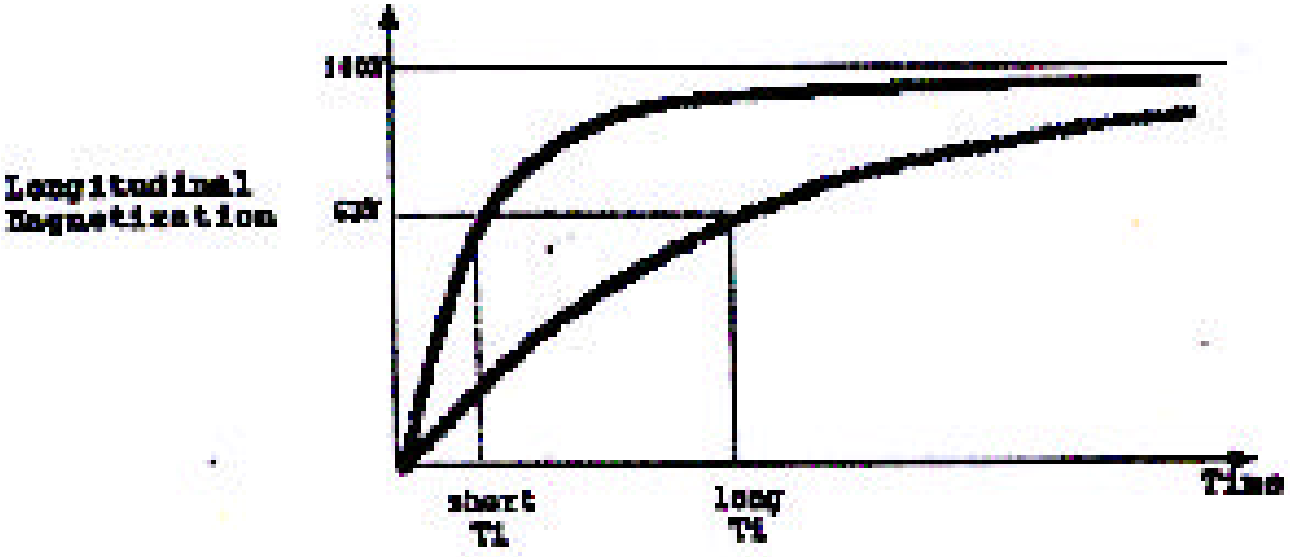


FIGURE 12. For two tissues, the longitudinal magnetization of the tissue with the shorter T_1 relaxation times regrows more quickly.

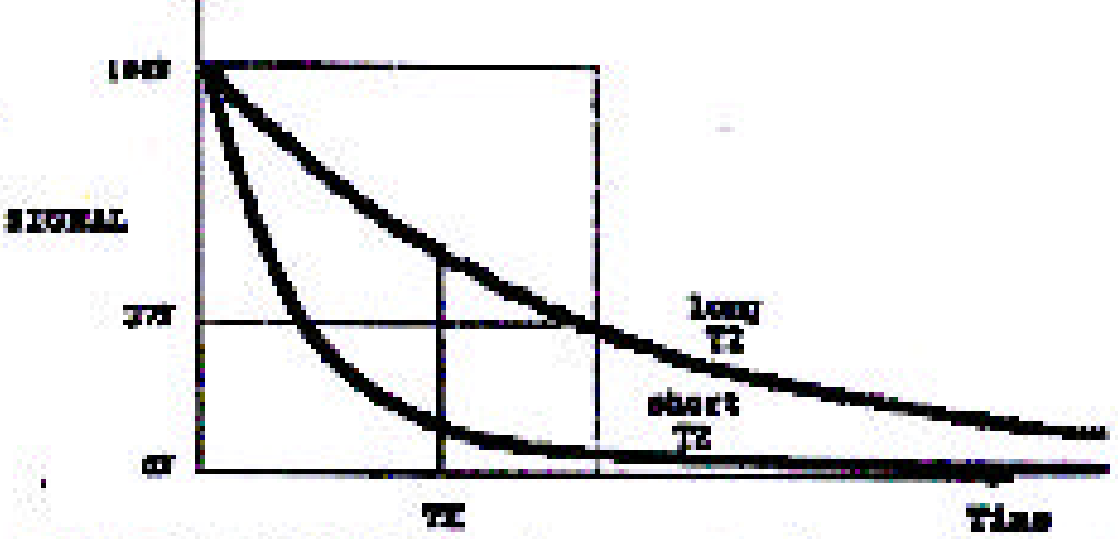


FIGURE 13. Signal strength versus time for two tissues with different T_2 relaxation times. Signal decays more slowly for the tissue with the longer T_2. Note that T_2 contrast initially increases and then decreases as the echo time (TE) is lengthened.

➔ The shorter the TR, the smaller the signal

➔ At fixed TR, area with shorter T1 will have stronger signal (T1 weighted Image)

➔ The Longer the Td, the weaker the signal

➔ At fixed Td, area with shorted T2 will have weaker signal (T2-weighted)

Different imaging modality.

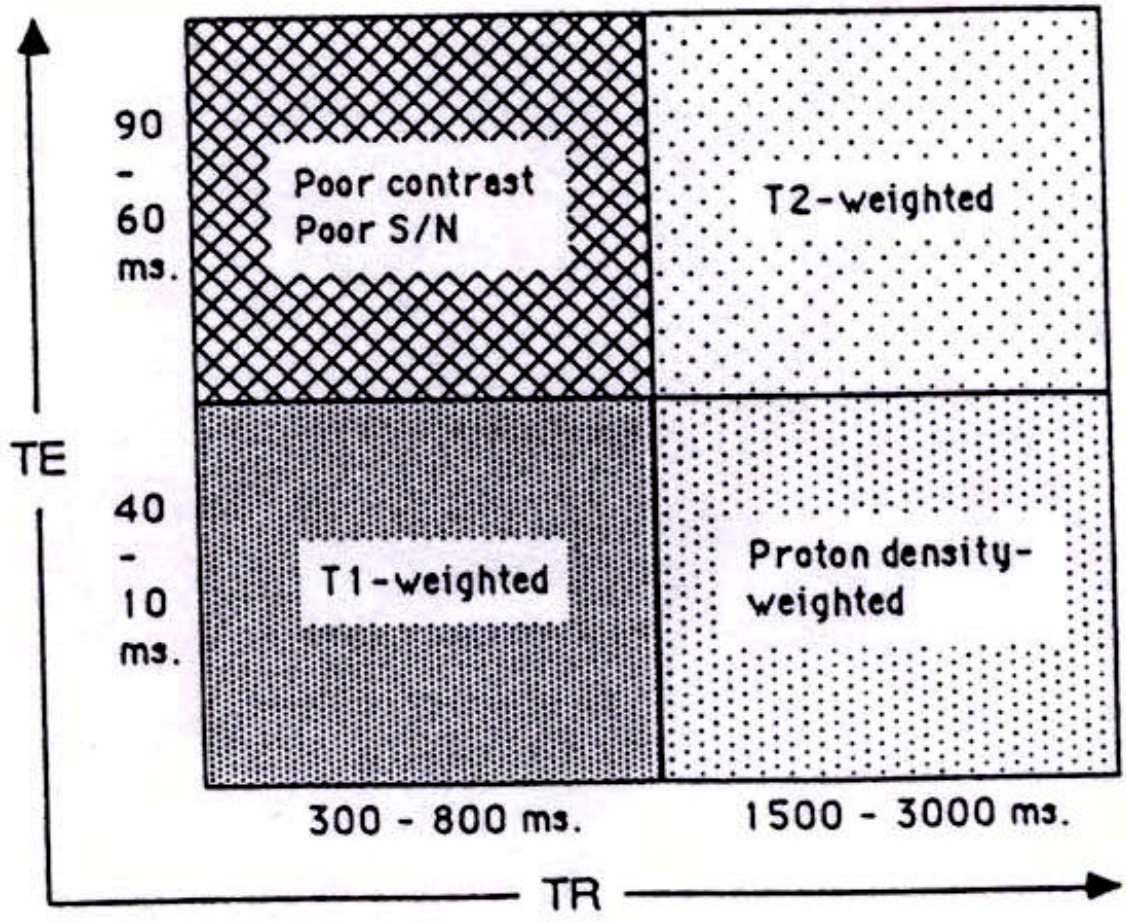


FIGURE 10. Simplified representation of image contrast as a function of TR and TE.

(f) T_1 weighted Images: Images acquired with short TR ($TR \sim T_1$) and short TE ($TE << T_2$). Signal intensity of tissues with long T_1 will be reduced.

(g) T_2 weighted Images: Images obtained with long TR and long TE ($TE \sim T_2$). Signal of tissues with short TE (Less mobil) will be attenuated.

(h) Proton Density-weighted Images: Images obtained with long TR ($TR >> T1$) and short TE ($TE >> T_2$). Images intensity will be proportional to the proton density of the tissue.

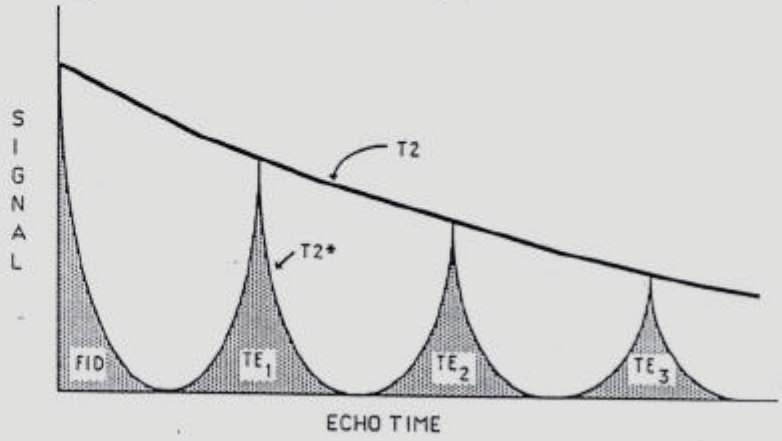


FIGURE 27. Signal decay in multiecho spin-echo acquisition.

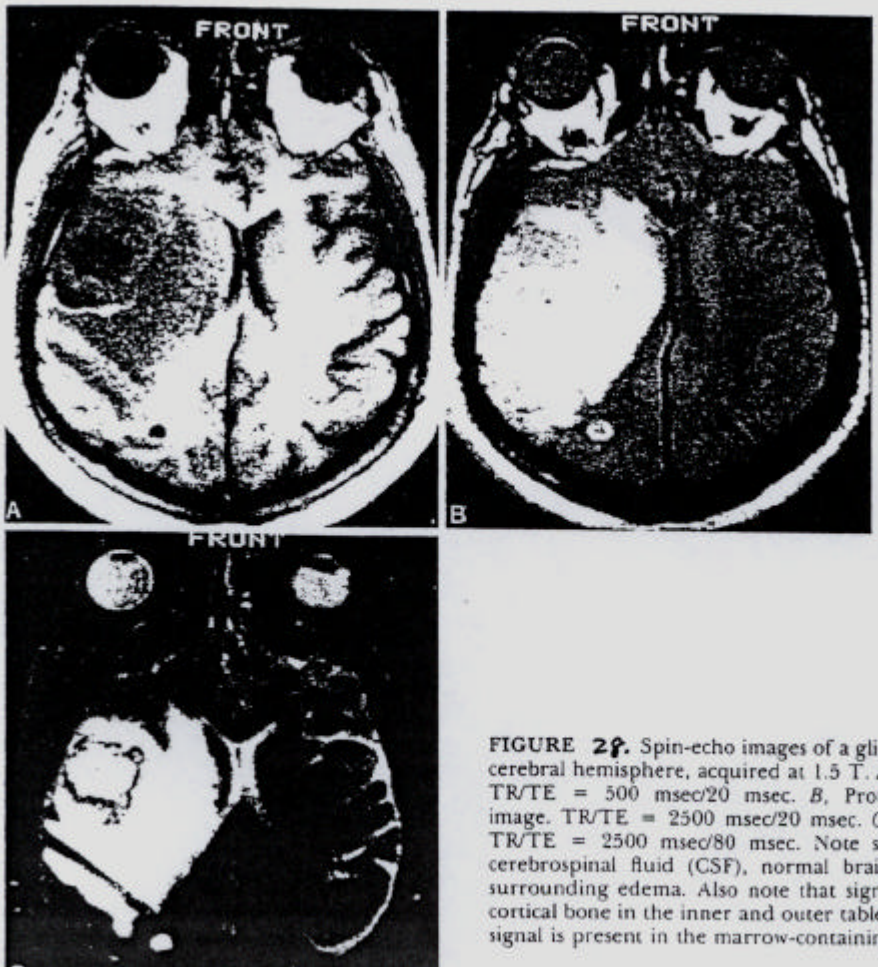


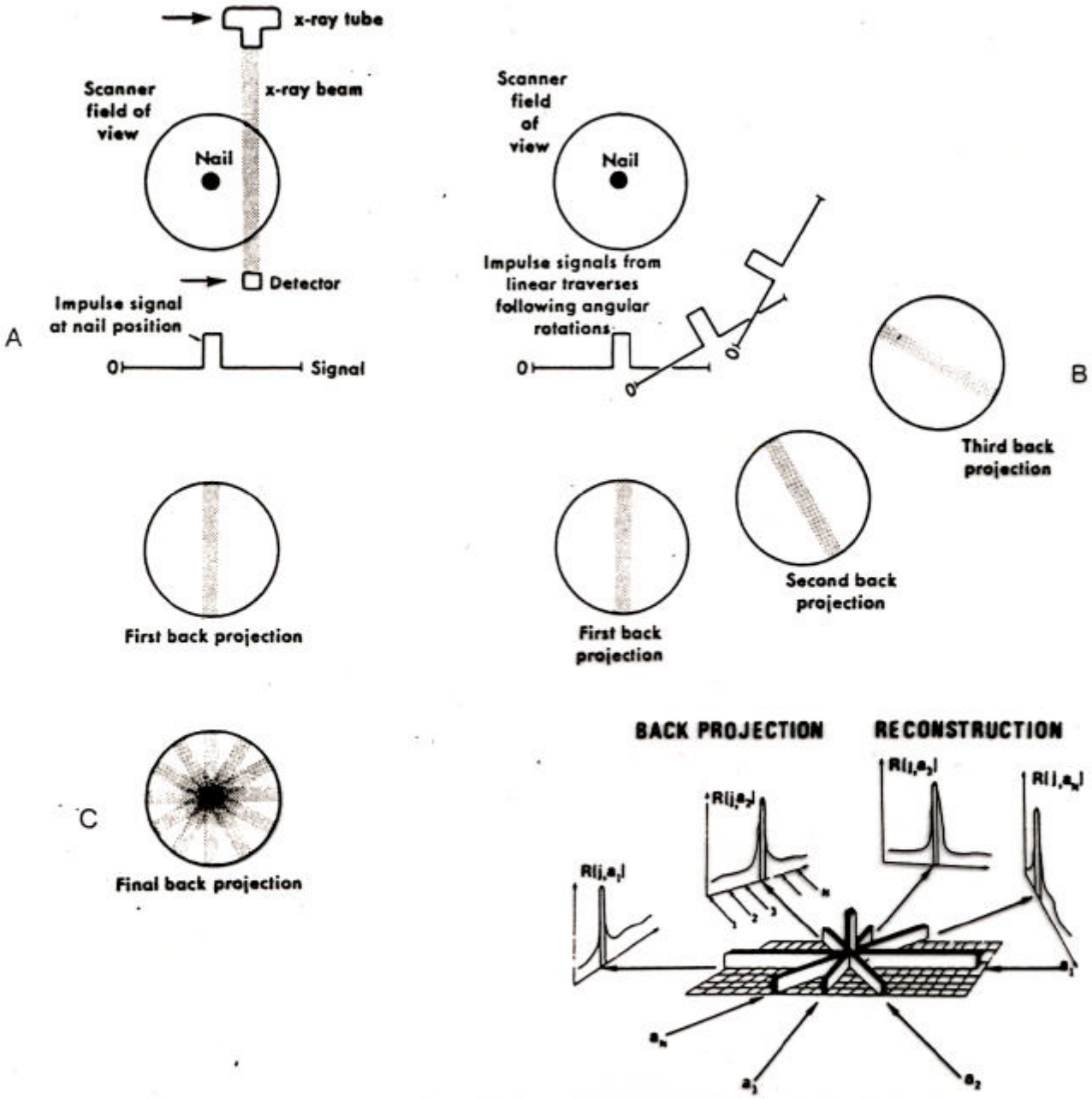
FIGURE 28. Spin-echo images of a glioblastoma of the right cerebral hemisphere, acquired at 1.5 T. *A*, T_1-weighted image. TR/TE = 500 msec/20 msec. *B*, Proton density–weighted image. TR/TE = 2500 msec/20 msec. *C*, T_2-weighted image. TR/TE = 2500 msec/80 msec. Note signal changes of fat, cerebrospinal fluid (CSF), normal brain, cystic tumor, and surrounding edema. Also note that signal is absent from the cortical bone in the inner and outer tables of the skull but that signal is present in the marrow-containing diploic space.

ON MR IMAGES

Tissue	T_1 Weighted	T_2 Weighted
Fat	Very bright	Intermediate-dark
Cysts		
Watery fluid	Very dark	Very bright
Proteinaceous fluid	Intermediate-bright	Very bright
Brain		
White matter	Bright	Mod. dark
Gray matter	Mod. dark	Mod. bright
CSF	Very dark	Very bright
Bone marrow		
Yellow	Very bright	Intermediate-dark
Red*	Mod. bright	Mod. dark
Cortical bone	Very dark	Very dark
Cartilage		
Fibrocartilage	Very dark	Very dark
Hyaline†	Intermediate	Intermediate
Intervertebral disk		
Normal†	Intermediate	Bright
Degenerated	Intermediate-dark	Dark
Osteophyte		
Marrow-containing*	Mod. bright	Intermediate-dark
Calcified only	Dark	Dark
Tendons/ligaments	Very dark	Very dark
Muscle	Dark	Dark
Lung	Very dark	Very dark
Liver		
Normal parenchyma	Mod. bright	Dark
Metastasis	Dark	Mod. bright
Hemangioma	Dark	Bright
Pancreas	Mod. bright	Dark
Spleen	Dark	Mod. bright
Contrast-enhanced tissue		
Gadolinium-DTPA		
Low concentration	Very bright	Bright
High concentration	Intermediate-dark	Very dark
Ferrite	Dark	Very dark
Fluosol	Very dark	Very dark
Blood flow	Bright or dark	Bright or dark
Hematoma‡		
Acute	Intermediate-dark	Dark
Subacute	Bright rim	Bright
Chronic	Dark rim, ± bright center	Dark rim, ± bright center

*Dark on phase-contrast proton density–weighted spin-echo or gradient-echo image.

†Bright on proton density–weighted gradient-echo image.



ure 5–47. The simple back projection reconstruction sequence is shown in these diagrams. *A*, A single projection of this body where only a single el is occupied is generated as previously described. The back projection assigns the same value to all pixels in this row. *B*, Scans at other ntations yield a set of back projections. *C*, These back projections are combined to yield a computer matrix of values. Display of these numbers a gray scale yields an image of the object, but one that has considerable star artifact. (Modified with permission of Coulam CM, Erickson JJ, et al: Physical Basis of Medical Imaging. East Norwalk, CT, Appleton and Lange, 1981, p 214; and of General Electric Co., Medical Systems Division, oduction to Computed Tomography, Milwaukee, 1976.)

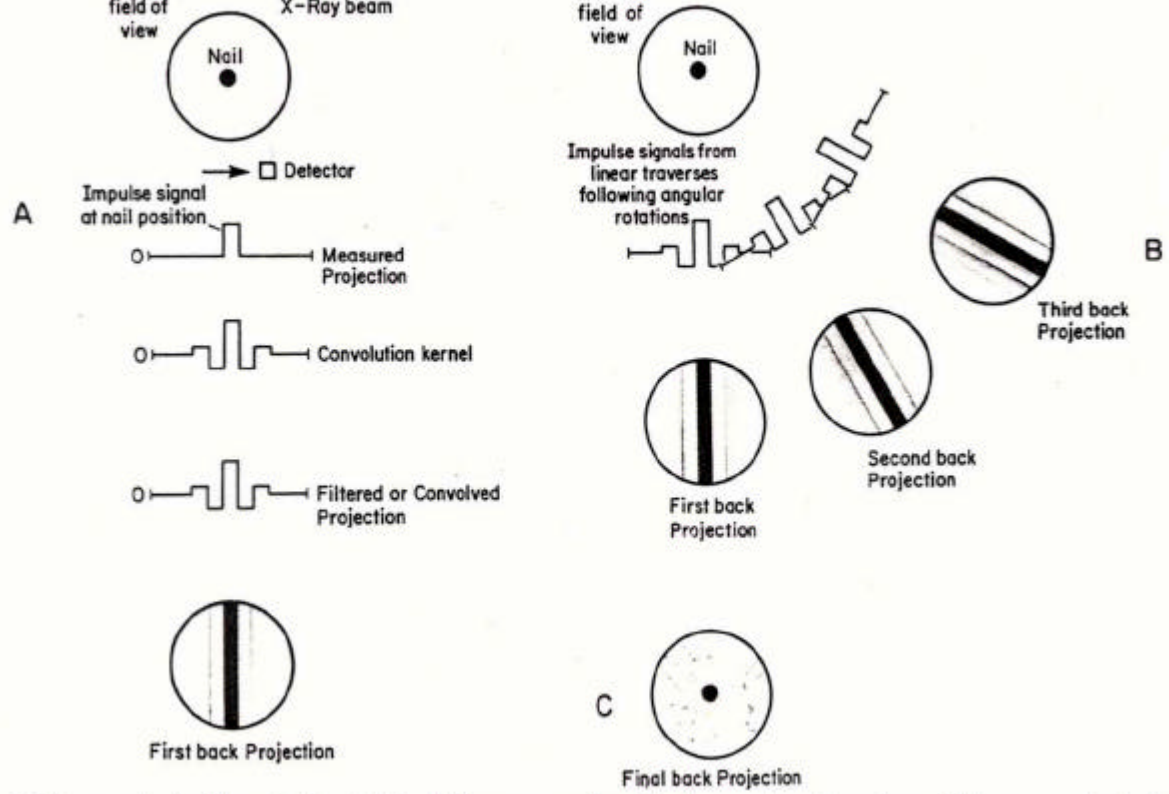
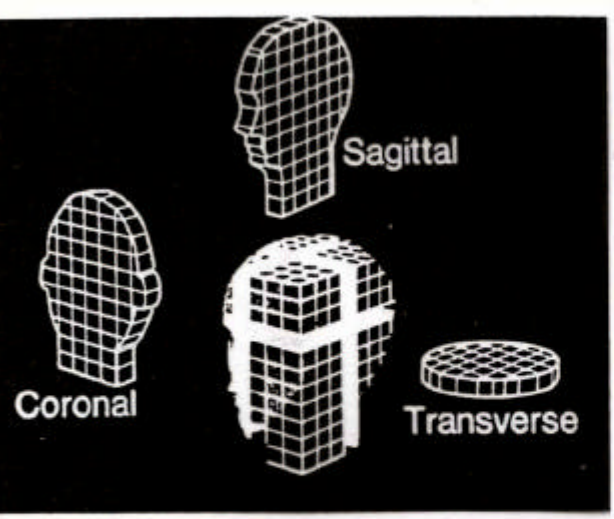


Figure 5–48. The convolved or filtered back projection eliminates star artifact with the procedures shown here. *A*, The measured projection is take as before, but each measured value influences not only the number in that location but also the neighbor locations by a mathematical process calle convolution. This process yields a filtered or convolved projection that is used in the back projection process. *B*, Multiple scans at other orientation yield a set of convolved projections. *C*, Summation of these "convolved" projections yields a final back projection in which star artifact is suppresse Most commercial CT scanners use this reconstruction process. The shape of the convolution kernel is sometimes altered for different application (Modified by permission of General Electric Co., Medical Systems Division: Introduction to Computed Tomography, Milwaukee, 1976.)



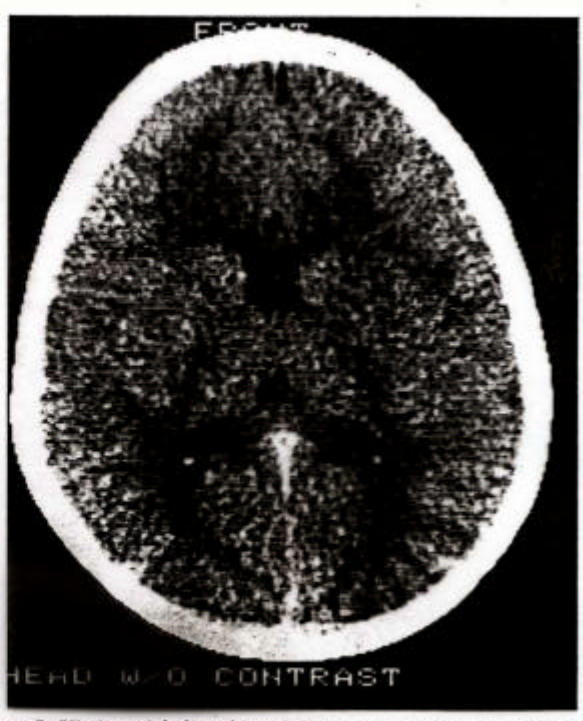


Figure 5–57. An axial slice through the basal ganglia area of the bra demonstrates the ability of CT to distinguish gray and white matter.

c. Spin-Warp Imaging Methods

(i) Slice selection: one gradient is applied with the RF pulse to choose a slice (Z-direction)

(ii) Frequency encoding: a second gradient is applied during detection period to locate the MR signal along one in-lane dimension. (x-direction)

(iii) Phase encoding: A third gradient is applied at fixed strength (or duration) between the slice selection and detection period to locate the other in-plane dimension. The strength (or duration) or the third gradient increases at constant amount for a total of N repetitive experiments so that the collective phase changes can be transformed to obtain spatial I formation of this dimension. (y-direction)

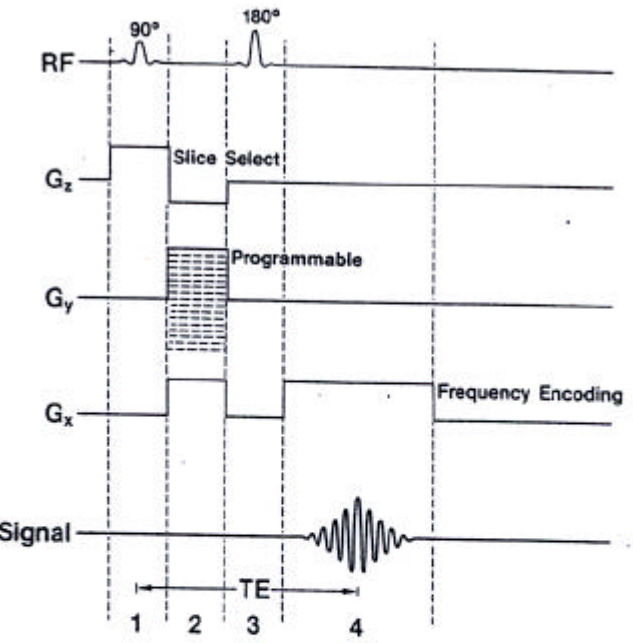


Figure 19. Pulse timing diagram for a typical 2DFT spin-warp imaging sequence. (See text for details.)

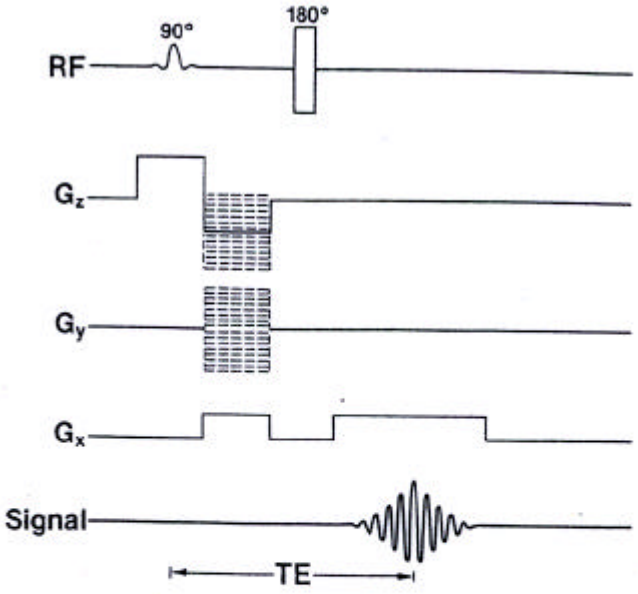
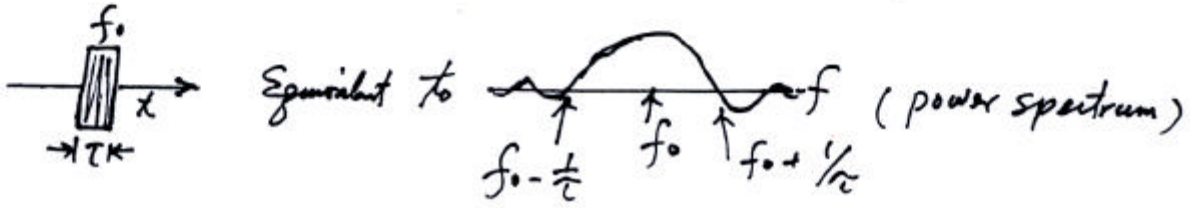


Figure 20. Pulse timing diagram of a typical 3DFT spin-warp imaging sequence. (See text for details.)



(i) Slice selection (Z-direction)

✻ Slice position:

Determined by the center frequency of the pulse and the gradient strength

$f(z) = r(B_0+ZG)/2p$

$$Z = (\frac{2pf}{g} - B_0)/G.....(5)$$

✻ Slice thickness:

Determined by both the pulse width and the gradient strength:

? $f = 1/t = ??Z\ G/2p$

$\therefore \Delta Z = 2p/?tG$……(6)

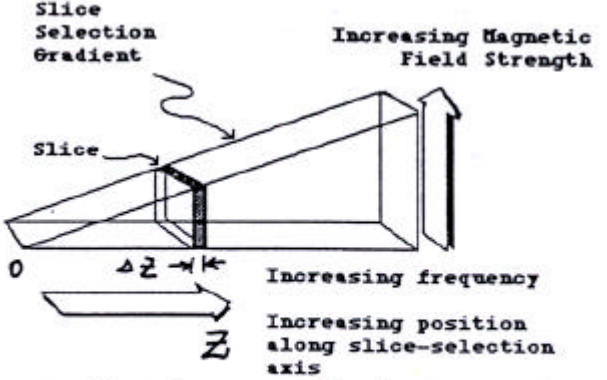


FIGURE 21. In the presence of the slice-selection gradient, the application of an RF pulse at a specific frequency excites tissue nuclei in a single slice.

$Z\mu\ 1/t,\ \ \Delta Z\mu\ 1/G$

Short pulse excite thick slice at fixed ΔG

Strong gradient give thinner slice at fixed τ

(ii) Frequency Encoding: (x-direction)

$G_x=0$ a and b resonate at same frequency

$G_x \neq 0$ a and b resonate at different requency

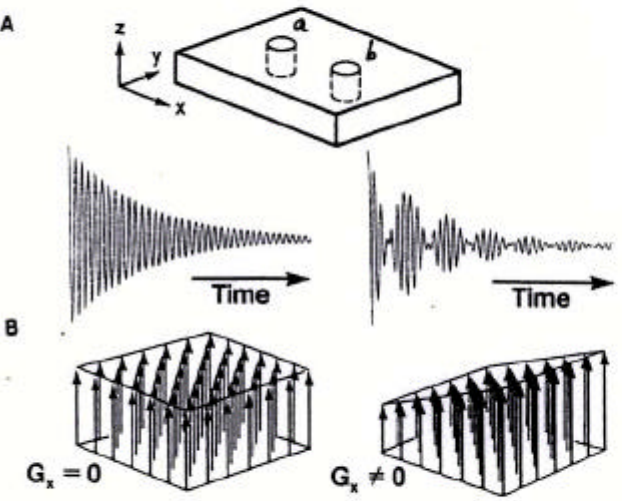


Figure 22. A, In the absence of the field gradient ($G_x = G_y = G_z = 0$) both samples sense the same field; the free induction decay therefore consists of a single frequency. B, In the presence of

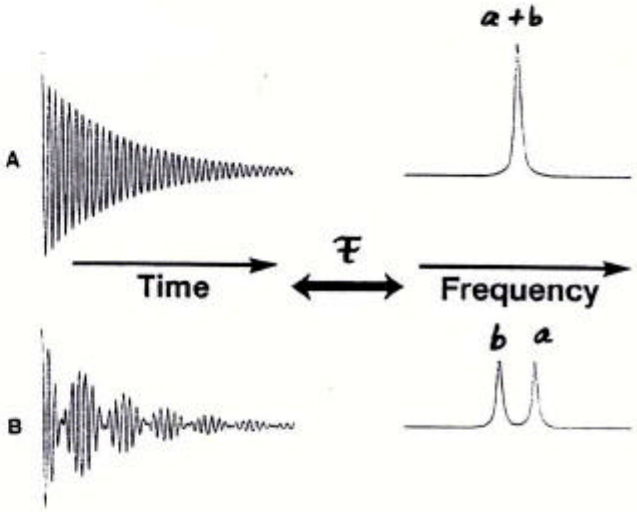
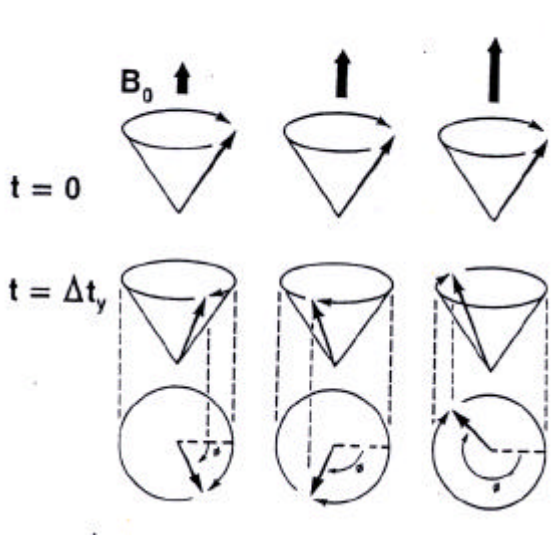
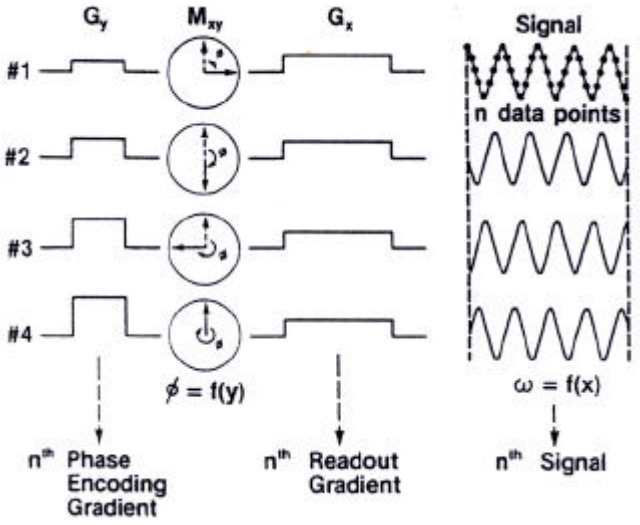


Figure 23. Free induction decay and its frequency domain analog for A, a single frequency and B, two different frequencies. The symbol *F* implies that the two domains are related by a Fourier transformation.

(iii) Phase encoding (y-direction)





In the presence of G_y (constant amplitude and duration for each repetition), spins at different y location will be resonating at different frequencies. Thus will accumulate different phase angle

$?_y(t)$: $?_r(t)=?G_yt$

Let $k_x=rG_yt$, $k_x=rG_yt$

Then the NMR signal S(x,y,z) :

$$S(x,y,z)= \int \int N(x,y)exp[-I(k_xx+ k_xy)]dxdy$$

The above scheme can be extended to three dimension such that

$$S(x,y,z,t)= \int \int \int N(x,y,z)exp[-I(k_xx+ k_xy+ k_zz)]dxdydz$$

(3-D FT imaging)

(i) Use G_z to select a slice perpendicular to z-direction

(ii) Use G_x is frequency encode magnetization along x-direction (same *f* at same *x*)

(iii) Use G_y to phase encode aling y-direction (same *y* same phase)

(iv) Repeat the experiment with different G_y

(v) 2-D Furier transform with respect to both *x* & *y* to get 2-D image of the slice

(vi) Change G_z (or f_0) to select different slice to obtain 3-D image

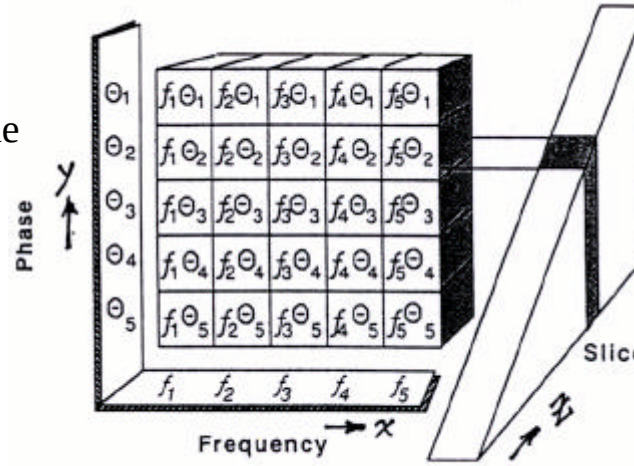


FIGURE 26. Summary of spatial localization in 2DFT imagin

(d) Signal overaging: NMR signal is usually weak. To increase signal to noise ratio (S/N) it is often necessary to repeat the experiment *n* time and add the signal together. S/N will increase by:

$S \propto n$ but $N \propto \sqrt{n}$ $\therefore S/N \propto \sqrt{n}$

Example: If S/N=0.5 for one scan, then for $n=100$

$S/N = 0.5 \times \sqrt{100} = 5$

(e) Imaging time for each slice:

$t = (TR) \times n \times (\text{number of lines}) = 1.0 \times 4 \times 128 = 512 \text{ seconds} \sim 8.4 \text{ minutes}$

Number of averaging scans

Repetition time ~ 1.05

a. Field of view (FOV): The length in each dimension, D_x, D_y and d of the image. d is the slice thickness.

b. Pixel: The smallest rectangle of a two-dimensional digital image.

$$\text{Pixel area} = (D_x/N_f)(D_y/N_p)$$

c. Voxel: The smallest volume of a three-dimensional digital image.

$$\text{Voxel volume} = \text{Pixel area} \times d = (D_x/N_f)(D_y/N_p)d$$

d. Signal-noise-ratio:

$$\text{SNR (or S/N)} \sim [D_xD_y(N_{acq.})^{1/2}/(N_fN_p\Delta F_{BW})^{1/2}][\omega^2/(a\omega^{1/2} + b\omega^2)^{1/2}]$$

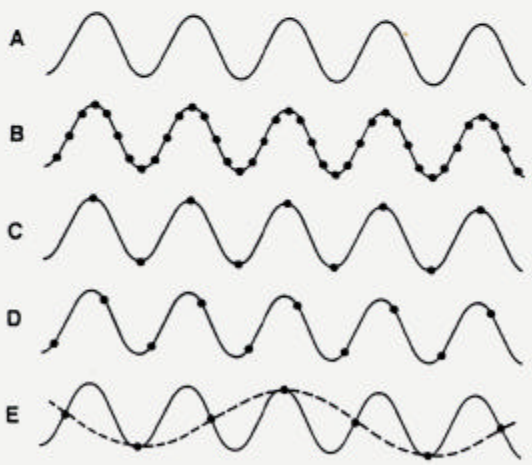
where ΔF_{BW} is the bandwidth of the sampling frequency, ω is the resonance frequency and N_{acq} is the number of averaging per spectrum.

e. Resolution of an image is usually expressed as pixel or voxel sizes.

(j) Nyquist Theorem: When sampling a periodic function one must sample at least twice as fast as the desired frequency, i.e. one need at least two points per period to define a epriodic wave otherwise aliasing will result.

$$N_f = 2/\Delta F_{BW}(x) = 4\pi/[\gamma G_x D_x] \quad \text{or} \quad G_x = 4\pi/[\gamma N_f D_x]$$

$$\textbf{similarly:} \quad N_p = 2/\Delta F_{BW}(y) = 4\pi/[\gamma G_y D_y] \quad \text{or} \quad G_y = 4\pi/[\gamma N_p D_y]$$



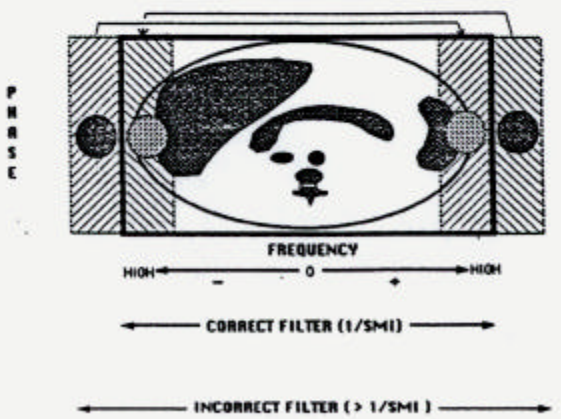


Figure 29. A continuous periodic signal can be recovered by interpolating between its discrete samples if at least two equally spaced samples are present in each cycle. A continuous signal is shown in A. The signal need not be sampled as often as in B. Two samples per cycle are acquired in C and D. In both cases the curves interpolated between the samples represent the continuous signal perfectly. Comparison of C and D shows that the positioning of the samples is irrelevant, provided that the samples are equally spaced and occur at least twice in each cycle. The

II. Instrumentation

1. magnet:

a. Permanent magnet (< 0.2 T, 1 T = 10,000 Gauss):
- -- Iron magnet: 23 tons.
- -- Neodymium alloy: 900 pounds.
- -- Normally operate at < 0.1 T.

b. Resistive Magnet (< 1.5 T):
- -- An electromagnet in which the magnetic field is generated by the passage of electric current.
- -- Requires high power, highly stable DC power supply (~ 50kW to generate 0.15 T field strength).
- -- Need water cooling.

c. Superconducting Magnet (~ 19 T):
- -- Nb/Ti is the most often used (T_c = 10K).
- -- Very high field is possible.
- -- Need liquid helium and liquid nitrogen cooling.
- -- Very stable.
- -- Has the potential of quenching.

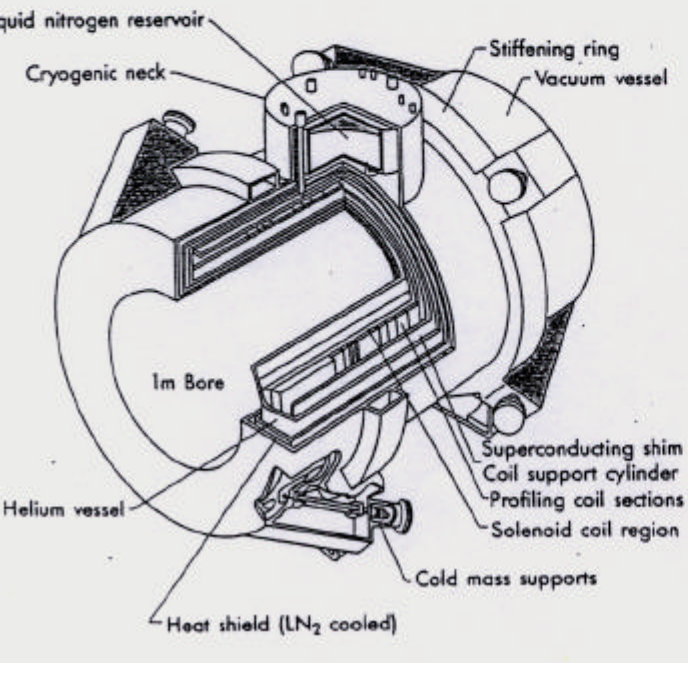
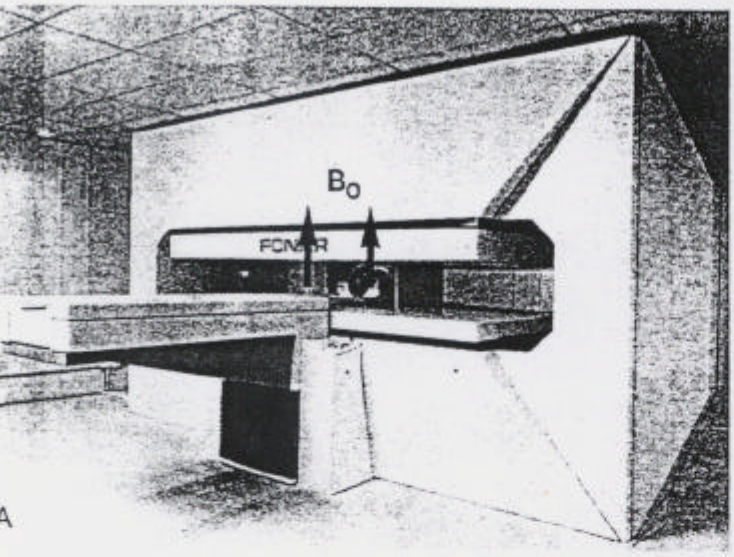


Figure 30. Superconducting magnet. A wire containing fila ments of Nb/Ti alloy embedded in a copper matrix are wound tightly and precisely on an insulated aluminum bore tube and fixed in place with a viscous, high thermal conductivity epoxy binder. Thousands of turns of the wire may be 30 km long and have several interconnecting joints, since it is not practical t wind the coil with a single continuous strand. The coil is coole to liquid helium temperatures by a surrounding can of liquid he lium, which is buffered from heat exchange with the surround ings by radiation shields, and a can of liquid nitrogen, whic boils at ~80° K and has 10 times the heat of vaporization of th more expensive liquid helium. The liquid nitrogen and radiatio shields reduce the boil-off of liquid helium to ~0.3 L/hour for typical 1 meter bore magnet (the nitrogen boil-off is ~ L/hour). (Courtesy S Burnett and J Purcell.)



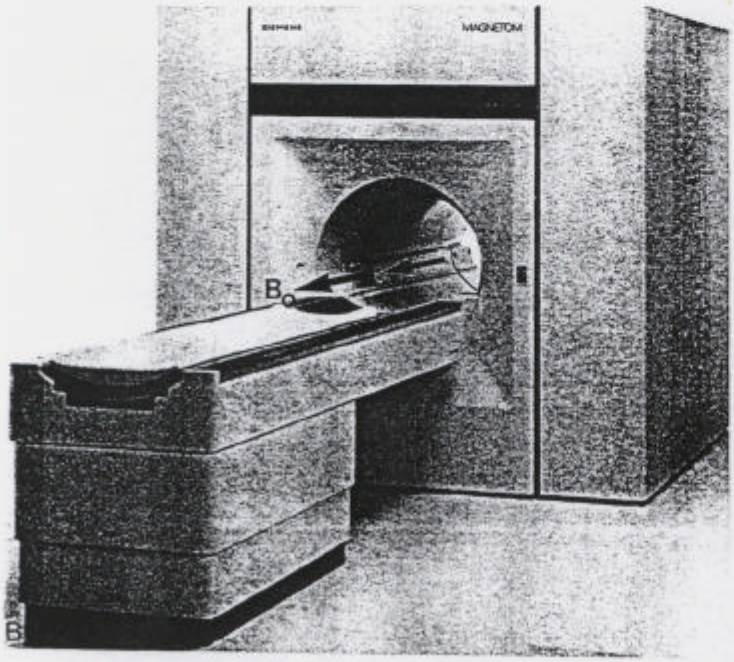


FIGURE 31. Main magnet field (B_o) direction is different for (*A*) permanent magnet and (*B*) superconducting magnet.



FIGURE 32. Comparison of image quality at different fie strengths using same pulse sequence and scan parameters. To = 0.5 T; middle = 1.0 T; bottom = 1.5 T.

A compound tagged with a positron-emitting nuclide such as ^{11}C, ^{18}F, ^{15}O, ^{13}N is administered to the subject either by inhalation or injection. Inside the body, a positron ejected from the radionuclide travels no more than a few millimeters before it encounters an electron. The resulting annihiliation produces two γ-ray photons, which shoot off nearly opposite (180°) directions. These γ-ray photons are detected by coincidence detectors located 180° apart on a rotating assembly. The only annihiliation events registered are those occuring within a volume defined by straight lines joining paiced detectors. A computer is used to reconstruct the spatial distribution of these annihilation events. It then can create cross-sectional images of the radionuclide's distribution in the organ or tissue being examed.

MRI:

Thermography:

Measurement of the infrared radiation from the skin constitutes the imaging specialty known as thermography.

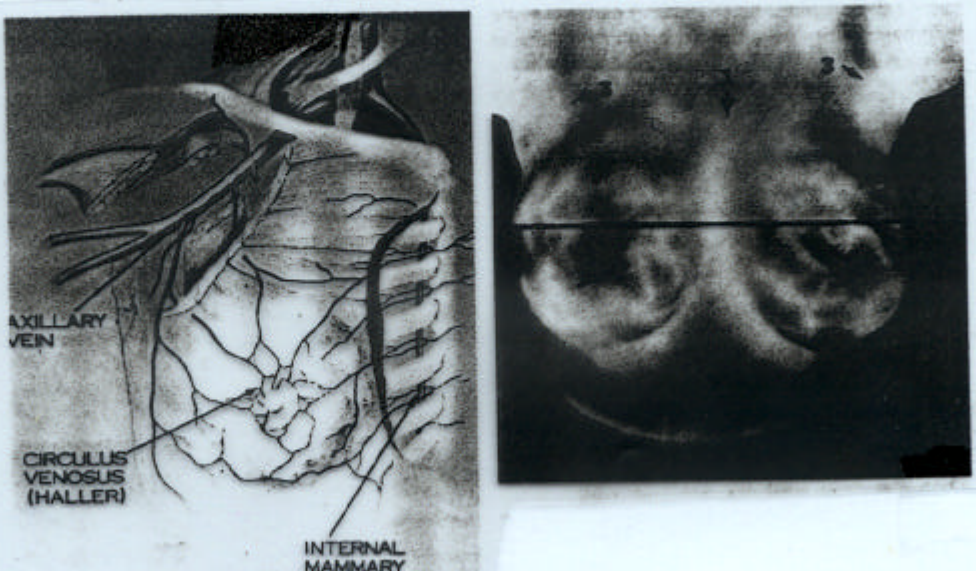


Figure 1–8. Infrared thermographic image of normal breasts. 1, Internal mammary vein drainage area. 2, Circulus venosus. 3, Axillary vein drainage area. (Reprinted with permission from Chang CH, Sibala L, Martin L: Breast thermography: Identification of differential vascular patterns in breast carcinoma. Acta Thermogr 2:138–142, 1977.)

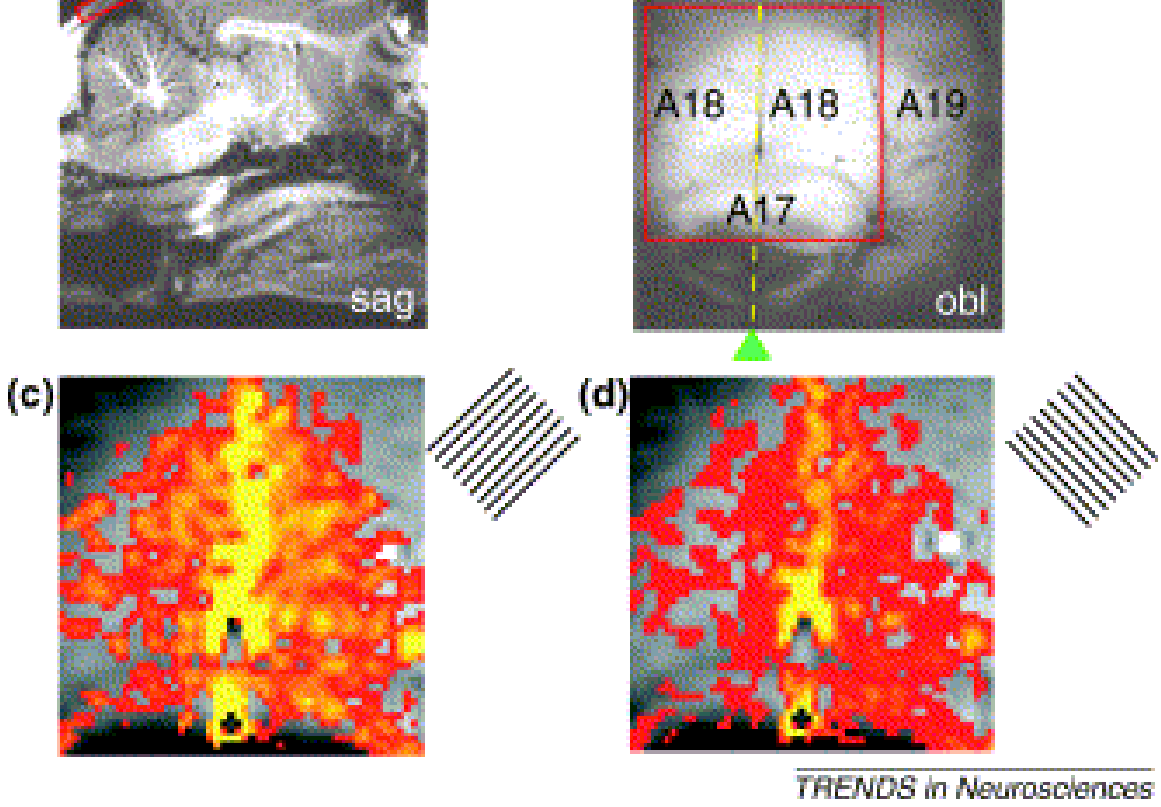


Fig. 1. Functional magnetic resonance (fMRI) images in cat primary visual cortex during stimulation of the animal with moving gratings of two different orientations, 45 °and 135 °. (a) Imaging slice showing the cat brain in sagittal (sag) view. (b) Image obtained from the oblique (obl) slice marked in red in (a), using T2* blood-oxygen-level dependent (BOLD) weighted fMRI acquisition scheme (nominal resolution, 156 ×156 m2). The dotted yellow line highlighted by a green arrow marks the space between the two hemispheres of the brain, the inter-hemispheric fissure, where the large blood vessel of the sagittal sinus is located. Images obtained after stimulation with a grating at 45 °or at 135 °are shown in (c) and (d), respectively. The colored pixels in (c) and (d) depict the regions of increased conventional T2* BOLD signals. Robust and homogenous activities were observed in the lateral gyri of both hemispheres. Note, however, that regardless of the stimulus orientation presented, the region of activity extended several millimeters in the anterior–posterior and medial–lateral directions, with the highest BOLD activity originating from the sinus sagittalis Consequently, the maps obtained for the different orientations

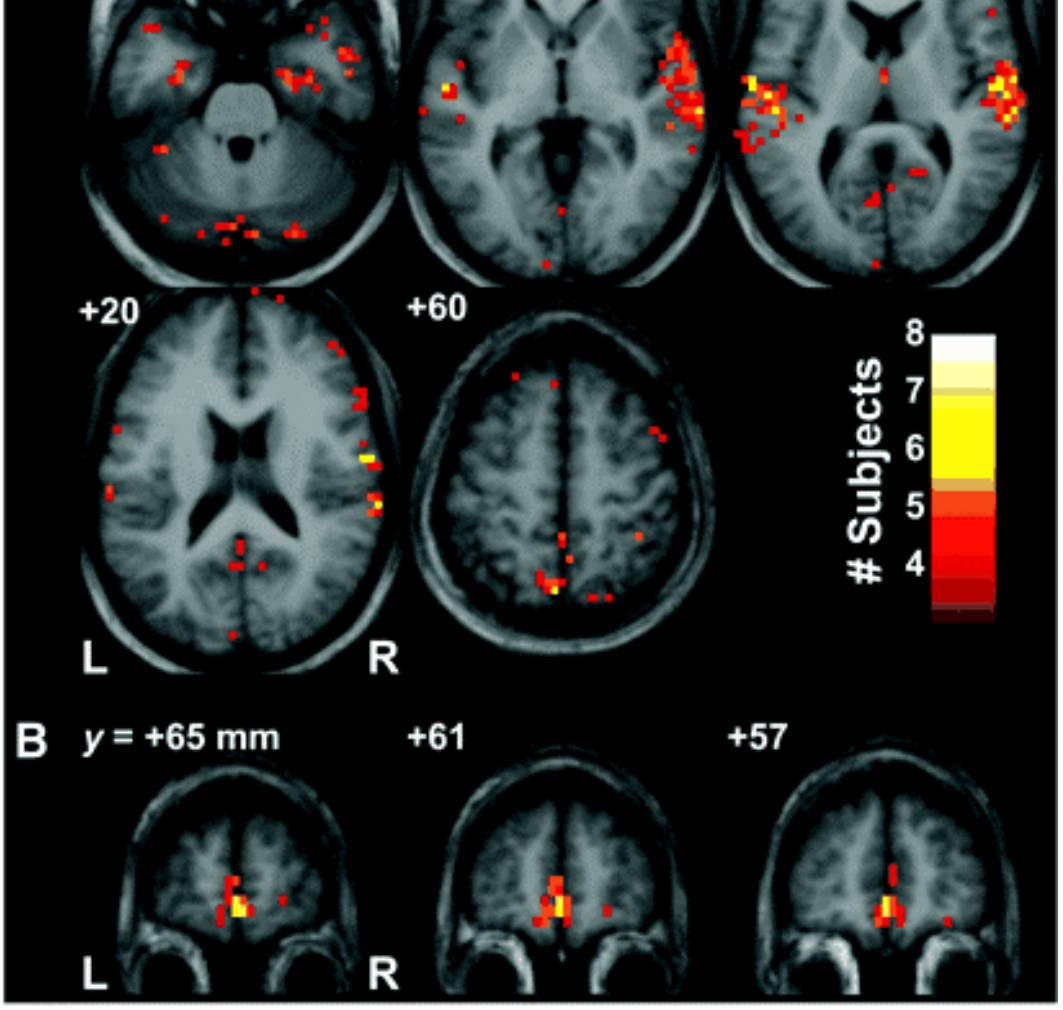


Figure 2. Group conjunction maps showing the consistency with which specific structures were activated across listeners. Conjunction maps of individual listeners, containing the voxels that were activated significantly ($P < 0.001$) in all scanning sessions for that listener, were normalized into a common space and summed together across listeners (see "spatial normalization" in supporting online text). Voxels that were consistently activated by at least four of the eight listeners are projected onto the group's mean normalized T1 image. (**A**) Areas sensitive to the two task regressors (Table 1). (**B**) The only areas whose activity patterns were significantly and consistently correlated with the tonality regressors both within and across listeners were the rostral portion of the ventromedial superior frontal gyrus and the right orbitofrontal gyrus.

Magnet	Positives	Negatives
Permanent magnet	No electric energy for operation Low capital cost Low operational cost High patient acceptance Low fringe field	Limited field strength Spectroscopy not possible Low SNR Field sensitive to temperature fluctuations
Resistive coil	Low capital cost Reliable No refrigerants Field can be readily and inexpensively turned on and off Variable geometry Easy siting and installation	Limited field strength High electric power consumption Spectroscopy not possible Low SNR
Superconducting coil	High fields (0.35-2 T) readily attainable High field homogeneity, 0.1 ppm attainable High SNR Spectroscopy possible Fast scanning supported by high homogeneity and high SNR	High capital cost Large fringe fields Expensive refrigerants must be replaced regularl Elaborate siting and high site preparation costs Quenches possible Patient claustrophobia Field cannot be readily turned on and off

d. Magnetic field shimming system: External resistive coil sets to improve the magnetic field homogeneity.

e. Field homogeneity and quality of images:

ppm / volume , Hz / cm

(ppm : part per million)

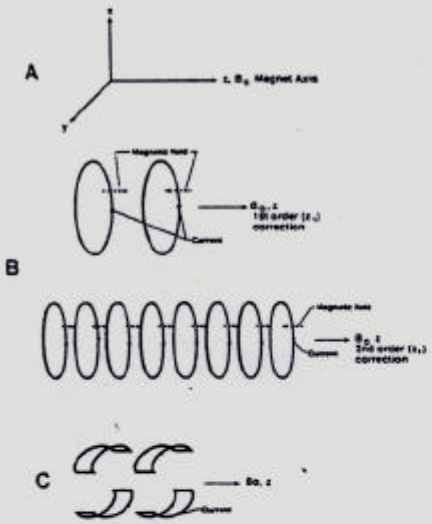


Figure 33. Shapes of shim coils for adjusting homogeneity of the B_0 field in axial and transverse directions. Coils are of varying orders of complexity and influence on the B_0 field. Higher order coils are of more complex field shape and smaller influence on the static B_0 field. Only first- and second-order axial shims and a first-order transverse shim are shown. Ordinarily, shim

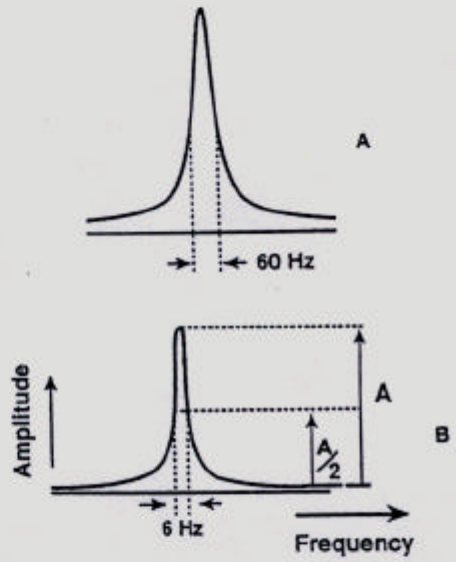


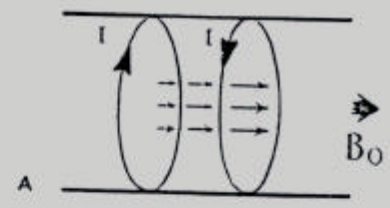
Figure 34. Line shapes of water proton resonance of brain of patient, obtained at 1.5 T. A, Inhomogeneous magnetic field. Water proton resonance is spread over a wide range of frequencies (ν). Width of line $\Delta\nu_{1/2}$ at half-the-maximum signal intensity (A/2) is 60 Hz. Frequency spread of the resonance is related to the time constant of the free induction decay (FID) by Fourier transformation. A large spread in the frequencies is characterized by a small time constant for the FID: $\pi\Delta\nu_{1/2} = 1/T2^*$ where T2* (5.3 ms = $1/\pi$ 60) is the time constant for the FID due to field inhomogeneities ($T2_{inh}$) and spin-spin relaxation (T2) ($1/T2^* = 1/T2_{inh} + 1/T2$). B, Magnetic field in A shimmed to homogeneity by minimizing water proton line width and optimizing its shape. Width is 6 Hz, which corresponds to T2 of 53 ms, close

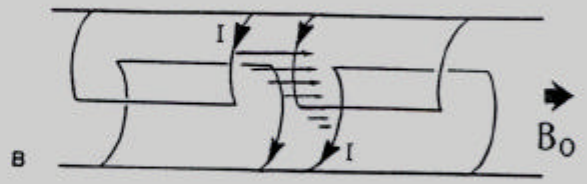
strength. For G = 1 gauss/cm (4257 Hz/cm) and a 1 x 1 mm voxel the homogeneity over the voxel must be better than 4257 Hz/cm x 0.1 cm = 425.7 Hz.

For a MRI system at 1.5 T this equivalent to (1G/cm)/(1.5 x 10,000 G) = 66.7 ppm/cm. But at 0.35 T this corresponds to only 28.9 ppm/cm (Check it out !). Normally one might like to have 10 time better homogeneity to see clear edges. In spectroscopy better resolution (< 0.1 ppm over the whole FOV is needed)

2. Gradient system:

-- At least three sets of gradient coils are needed.
-- Things to consider in gradient coils:
  a. Strength (> 1G/cm).
  b. Switching time (< 1ms).
  c. Eddy current: Can be compensated by: preemphasis or active shield.





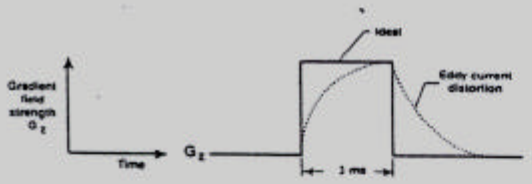


Figure 35. Time profile of an ideal rectangular gradient pulse and one distorted by eddy currents (and magnetic fields) induced in surrounding conductors.

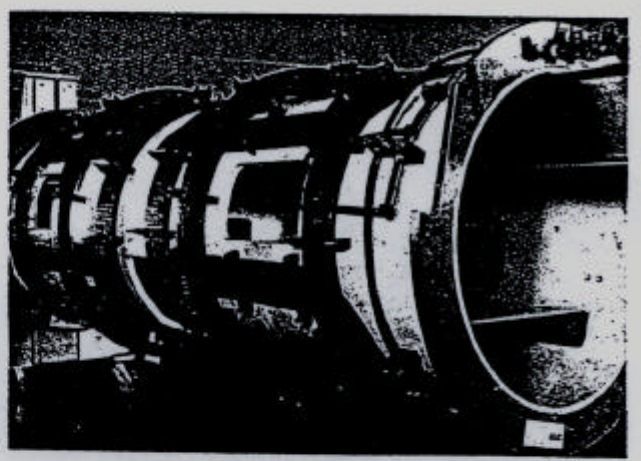


Figure 36. Typical gradient coil configurations used to produce gradients that are parallel (A) and perpendicular (B) to the static field B_0. Configurations shown are a Maxwell pair (A) and Golay coils (B). Arrows represent fields produced by the gradient coils superimposed on the larger B_0 static field. Differences in field strength (i.e., gradient, as indicated by differences in length of the arrows) are considerably exaggerated over those found in actual systems (i.e., B_0 is typically 10,000 gauss and the field gradient is on the order of 1 gauss/cm). C, Gradient coils for a superconducting magnet. These fit within a 1-meter cryostat bore, reducing the diameter available for RF coils and patients

a. Coils:

-- For transmitting and receiving RF signals.

-- Volume coil and surface coil.

-- Quality factor (Q) determines the sensitivity of the entire MRI system.

-- $Q = 1/r\omega_0 C$ where r n is the coil resistance, ω_0 is the resonance frequency and C is the coil capacitance.

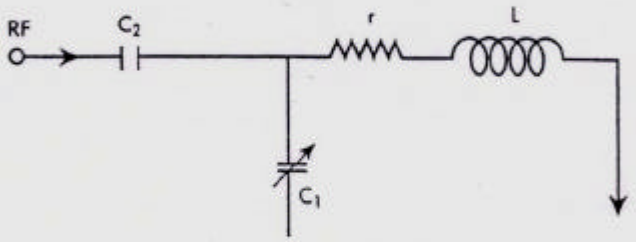


Figure 37. An RF coil is equivalent to an electric circuit having an inductance (*L*), a capacitance (*C*), a resistance (*r*), and a voltage oscillating at frequency ω. Peak current in the circuit (and in the coil magnetic field) will occur when $\omega = 1/\sqrt{LC}$ (if $r << \omega L$, a condition easily met). This is accomplished by adjusting C to achieve the resonance condition for the circuit (and the coil). Note that for MRI, ω of the coil is the precessional frequency of nuclear spin moments. C_1 denotes an external capacitor that can tune the circuit to resonance.

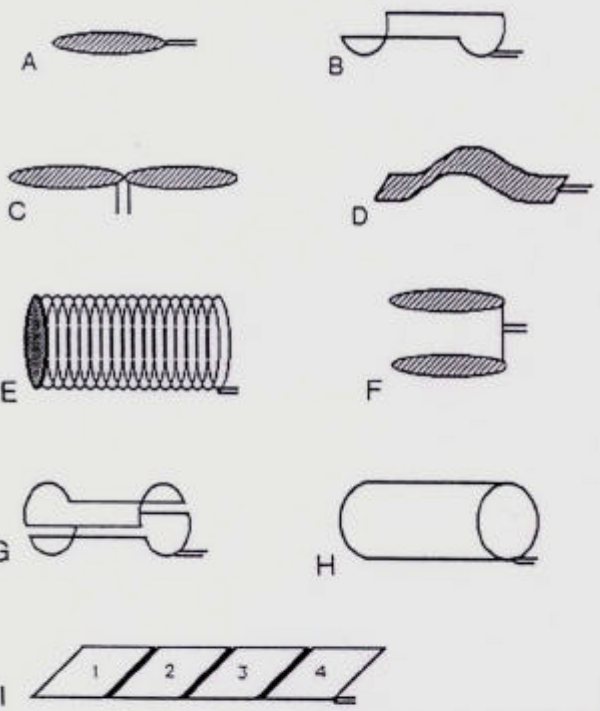


FIGURE 38. Schematic drawings of various receiver coils. *A*, Flat surface coil used for spine imaging. Small versions may be used for orbit imaging. *B*, Half-saddle coil used for neck imaging. *C*, Butterfly coil for spine imaging. *D*, Flexible coil for neck imaging. *E*, Solenoid coil used for head and extremity imaging in permanent magnet systems. *F*, Helmholtz pair used for neck and shoulder imaging. *G*, Saddle coil used for head imaging at low to mid field strengths. *H*, Resonator coil used for head and extremity imaging at high field strengths. *I*, Ladder coil for total spine studies.

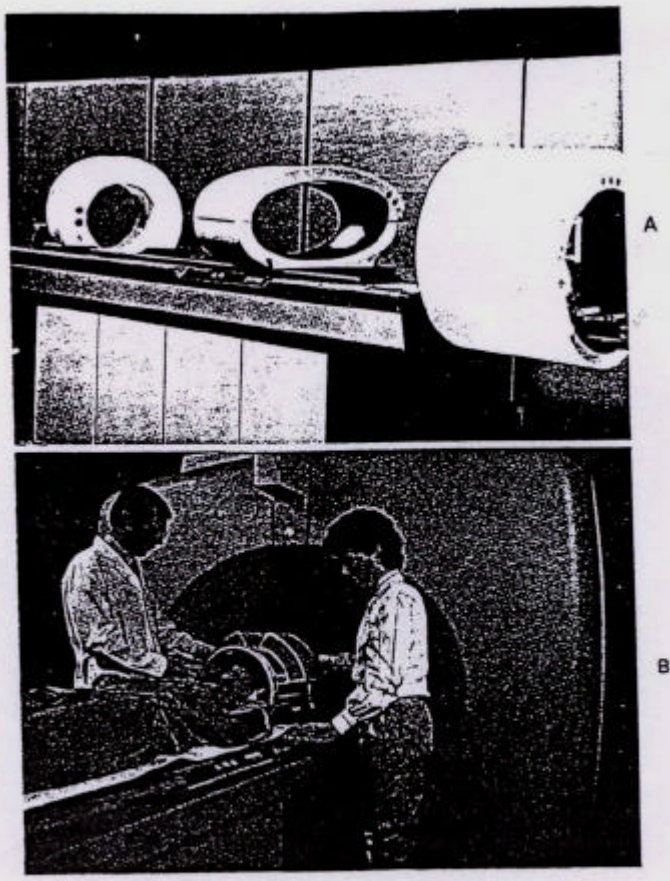


Figure 39. Small volume coils. A, Saddle-shaped RF coils

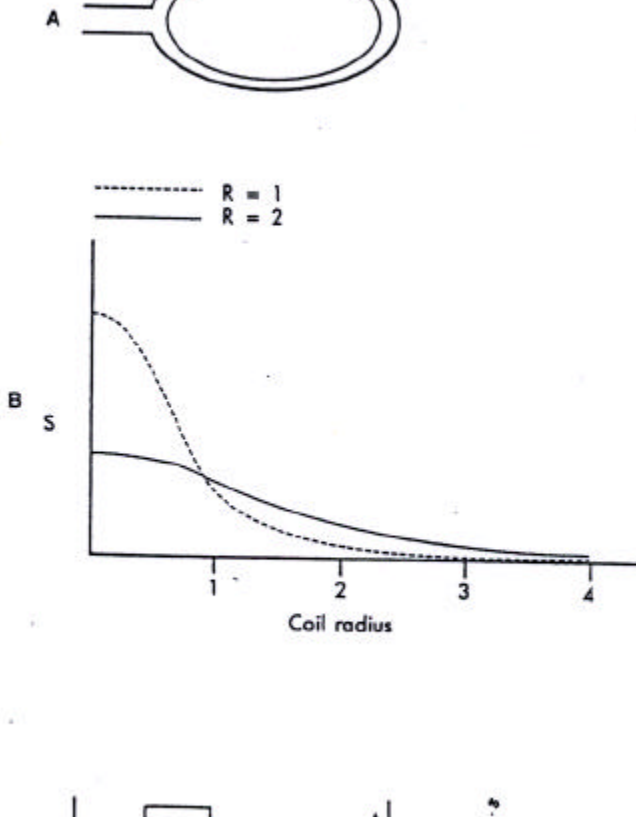


Figure 40. Schematic sensitivity profiles of single-loop circular surface coil. **A**, Geometry of the surface coil. **B**, Sensitivity of the surface coil for tissue MR signal and noise falls with distance from the coil, but a whole-volume coil has a uniform region of sensitivity. Axial signal intensity *(S)* versus tissue depth measured in coil radii. Sensitivity profile along line orthogonal to center of a receive-only, single-loop circular surface coil shows calculated effects of doubling the coil radius *(R = 2)*. For deep structures, the larger coil yields slightly better SNR, although the measured difference in SNR between the two coils is smaller than this calculation would indicate.

b. Transmitter system:

-- Power requirement.
-- Shaped pulse.

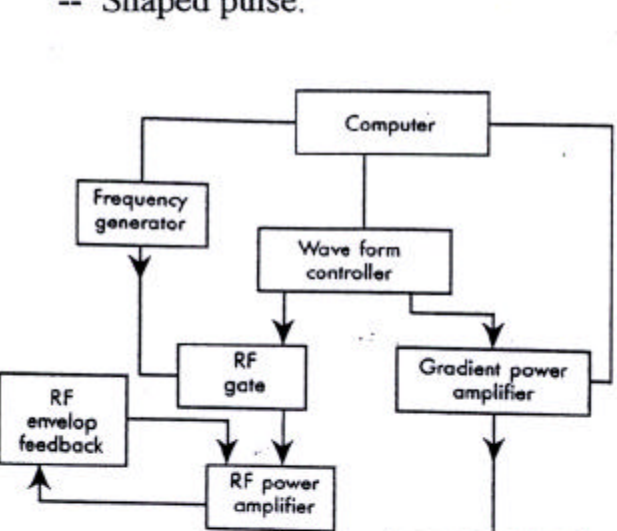


Figure 41. Simplified flow chart of the transmitter section of an MRI system. Reference frequency at low power is provided by an extremely precise and stable frequency synthesizer or a fixed frequency RF oscillator. The frequency generator not only generates the central RF frequency but also provides for small shifts in this central frequency to move from selected slice to new selected slice. The digital pulse shape is provided from the computer to the waveform controller, which passes this waveform through precisely timed RF gates to the RF power amplifier. Driven by the waveform generator, the amplifier generates the appropriately shaped frequency selective RF pulse of prescribed flip angle to the transmitter coil. It is critical that the energy from the power amplifier be transmitted efficiently into the RF coil. This requires that the antenna (the two circuits)

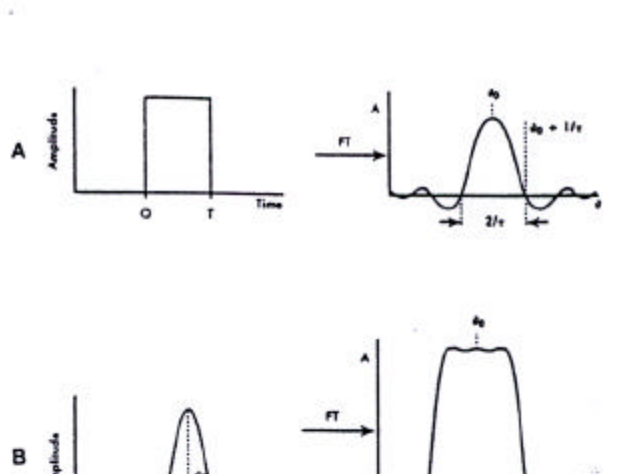


Figure 42. Shaping RF transmitter pulses to cover a specific frequency range. A, If an RF transmitter at the single frequency ν_0 is turned on at time t = 0 and then turned off after a few milliseconds T = τ, then FT analysis of the amplitude as a function of frequency reveals that output is not a single frequency ν_0, but the spread of frequencies shown. The amplitude of the B_1 field as a function of time is shown as it would appear in the rotating frame (see Figure 3-14), as a constant. If the rotating frame description were not used, as in Figure 3-20, *A (left)*, the operation would correspond to transmitting only a limited number of cycles of the oscillating RF wave. **B**, If the time-dependent amplitude waveform shown (*A* versus *t*) is imposed on the RF of frequency ν_0 shown in **A**, then FT analysis of B_1 in the frequency domain is an output such that magnetization flipped into the transverse plane has the shape shown—it rises and falls relatively sharply with ν and is centered about the frequency ν_0 with a bandwidth of $1/\tau$ Hz.

c. Receiver system:

-- Rotating frame system (Audio frequency detection).
-- Phase sensitive detection.

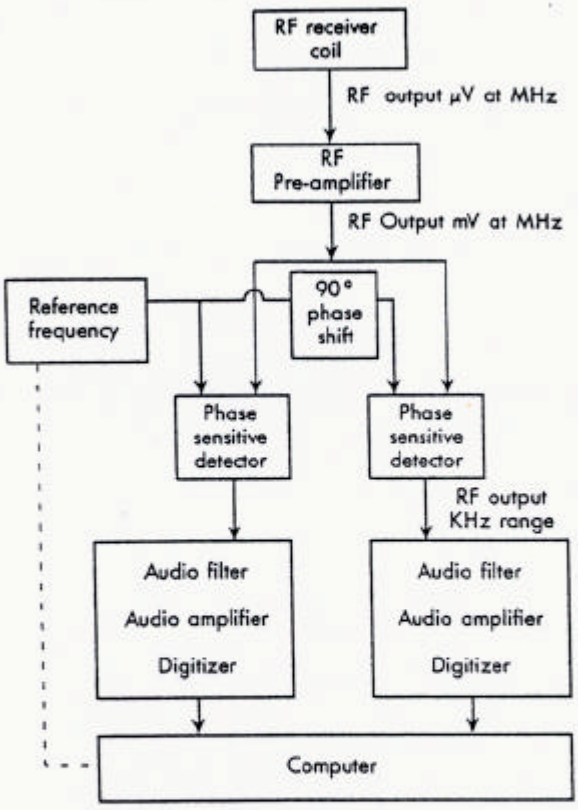


Figure 43. RF receiver system. The low level (μV) output of the receiver is amplified in a broad band, very-low-noise preamplifier (extra noise at this stage is disastrous). The amplified RF signal is then mixed with the reference frequency ν_T provided by a computer clock or frequency synthesizer generating the signals $\nu_T - \nu_i$, which are the difference audio signals detected by a quadrature detector. Audio signals are passed by an audio filter into a high-power audio amplifier and then digitized and stored in the computer.

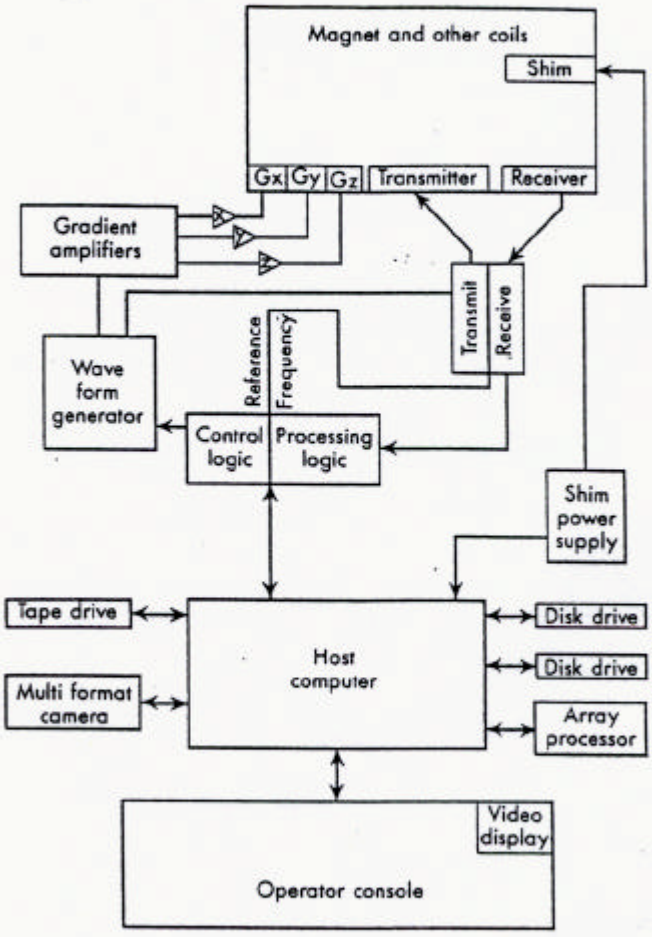


Figure 44. Simplified block diagram of a representative MRI system.

d.Computer system:

MRI QUIZ

(June 11, 1996)

Name: Score:

(Notice: All MRI is assumed to be detected in ^{1}H channel with γ =4257 Hz/G)

I. True (O) or false (X): (4 points each)

( ) 1. All nuclei possess nuclear spin, therefore are all NMR observable.
( ) 2. All isotope of the same element resonate at the same frequency.
( ) 3. For a given nucleus, the higher the static field the higher the resonance frequency.
( ) 4. T_1 is also called transverse relaxation time.
( ) 5. The more mobile tissue has longer T_2.
( ) 6. From the decay rate of an FID one can measure T_2.
( ) 7. The relaxation of magnetization in the Z-direction is called a T_1 process.
( ) 8. A T_2-weighted image is obtained with long TR an long TE.
( ) 9. When we apply a G_x gradient to the NMR sample in a uniform static magnetic field then all water protons in the X-direction will resonate at different frequency.
( ) 10. A short pulse will allow the selection of a thicker slice in a fixed gradient.
( ) 11. A stronger gradient allows the selection of thinner slice with a fixed pulse length.
( ) 12. During the detecting period a gradient is applied in a certain dimension. This gradient is called phase encoding gradient.
( ) 13. Aliasing is an artifact resulted from improper receiver filter setting.
( ) 14. A T_1-weighted image is obtained with short TR and short TE.
( ) 15. In a 2D spin-warp experiment the phase encoding gradient is fixed at a constant value.

II. Multiple choices (only one is correct): (4 points each)

( ) 1. Which of the following factors has no effect on NMR resonance frequency:
(a) magnetic field strength; (b) chemical environment; (c) magnetic field gradient
(d) RF-field strength.
( ) 2. If we average the signal 4 times the signal to noise ratio of the image will increase by a factor of: (a) 4; (b) 2; (c) 1/2; (d) 1/4.
( ) 3. To detect an image of FOV=10cm in a gradient of 1 G/cm the bandwidth of the receiver must be: (a) 4257 Hz; (b) 42570 Hz; (c) 4257 kHz; (d) 10Hz.
( ) 4. To obtain a T_1-weighted image in a spin-warp experiment one must set:
(a) Both TR and TE must be long; (b) TR~T_1 and TE very long;
(c) TR long and TE~T_1; (d) Both TR and TE very long.
( ) 5. In a T_2-weighted image which of the following is true:
(a) Signal of tissue with short T_2 will be attenuated;
(b) Signal of tissue with short T_2 will be enhanced;
(c) Signal of tissue with short T_1 will be attenuated;

must be: (a) 10 us; (b) 14.8 ms; (c) 67.5 us; (d) 10 ms.

( ) 7. Which of the following statement concerns MRI magnet is not true::

(a) The higher the magnetic field the better the image quality one can expect.

(b) Superconducting magnet has highest field homogeneity.

(c) Permanent magnet is the most stable magnet.

(d) The higher the field one use the higher the transmitter power one need.

( ) 8. Which of the following statement concerns MRI instrument is not true:

(a) molecular motion; (b) magnetic field strength;

(c) sample size; (d) temperature.

( ) 9. Which of the following factor is the least important in affecting MRI sensitivity:

(a) Magnetic strength; (b) receiver preamp noise figure;

(c) Coil Q factor; (d) transmitter power.

( ) 10. Calculate the pixel area of an image of 128 x 128 with FOV 10cm x 10cm:

(a) 100 cm^2; (b) 16384 cm^2; (c) 1280 cm^2; (d) 6.1 x 10^{-3} cm^2.